

Fe t_{2g} band dispersion and spin polarization in thin films of Fe₃O₄(001)/MgO(001): Half-metallicity of magnetite revisited

W. Wang,^{1,2} J.-M. Mariot,³ M. C. Richter,^{1,4} O. Heckmann,^{1,4} W. Ndiaye,¹ P. De Padova,⁵ A. Taleb-Ibrahimi,⁶ P. Le Fèvre,⁷ F. Bertran,⁷ F. Bondino,⁸ E. Magnano,⁸ J. Krempaský,⁹ P. Blaha,¹⁰ C. Cacho,¹¹ F. Parmigiani,^{8,12} and K. Hricovini^{1,4}

¹Laboratoire de Physique des Matériaux et des Surfaces, Université de Cergy-Pontoise, 5 mail Gay-Lussac, 95031 Cergy-Pontoise, France

²Institute of Precision Optical Engineering, Department of Physics, Tongji University, Shanghai 200092, People's Republic of China

³Laboratoire de Chimie Physique–Matière et Rayonnement (UMR 7614), Université Pierre et Marie Curie, 11 rue Pierre et Marie Curie, 75231 Paris Cedex 05, France

⁴DSM, IRAMIS, Service de Physique et Chimie des Surfaces et des Interfaces, CEA-Saclay, 91191 Gif-sur-Yvette, France

⁵CNR, Istituto di Struttura della Materia, via Fosso del Cavaliere, 00133 Roma, Italy

⁶URI-CNRS/Synchrotron SOLEIL, Saint-Aubin, B.P. 48, 91192 Gif-sur-Yvette Cedex, France

⁷Synchrotron SOLEIL, Saint-Aubin, B.P. 48, 91192 Gif-sur-Yvette Cedex, France

⁸CNR, Laboratorio TASC INFM, S.S. 14, Km 163.5 in Area Science Park, 34012 Trieste, Italy

⁹Paul Scherrer Institut, 5232 Villigen PSI, Switzerland

¹⁰TU Wien, Institut für Materialchemie, Getreidemarkt 9/165, 1060 Wien, Austria

¹¹Central Laser Facility, Rutherford Appleton Laboratory, Didcot, Oxon OX11 0QX, United Kingdom

¹²Department of Physics, Università degli Studi di Trieste, 34127 Trieste, Italy

(Received 18 October 2012; revised manuscript received 20 December 2012; published 14 February 2013)

We have performed angle- and spin-resolved photoemission measurements on Fe₃O₄(001)/MgO(001). Despite intrinsic electron-lattice (polaron) interaction a Fe t_{2g} band dispersion is observed, as well as a Fermi surface. The states close to the Fermi level show a spin polarization up to -72% as measured with a 4.65 eV laser light. All the data can be simulated starting from GGA + U bulk band-structure calculations and taking into account the polaron and initial-state lifetime broadening involved in the photoemission process. This conciliates the electronic structure of Fe₃O₄ with a band model and confirms the half-metallic nature of Fe₃O₄.

DOI: [10.1103/PhysRevB.87.085118](https://doi.org/10.1103/PhysRevB.87.085118)

PACS number(s): 79.60.-i, 71.20.-b, 75.25.-j, 71.18.+y

I. INTRODUCTION

Recently there is a growing interest in oxide interfaces, namely in artificially created structures involving magnetic transition-metal oxide compounds,^{1,2} because, for example, controlling ferromagnetism by an external electric field is a great challenge for material physics to develop low-power-consumption spintronics devices. In this perspective, a deeper understanding of the properties of magnetite (Fe₃O₄) can bring conceptual advances in these materials. Indeed Fe₃O₄ is very attractive as it exhibits robust ferrimagnetism (the Curie temperature is as high as ~ 850 K) and it has been suggested to be a half-metal (HM).³⁻⁵ In addition, it avoids problems related to oxidation when building electronic components, it is very stable, it does not constitute a health hazard, and it is cheap. As a consequence Fe₃O₄ has a great potential to serve in spintronic devices⁶ and multiferroics materials.⁷ Having detailed information on the distribution of charge and spin of the valence electrons in Fe₃O₄ is thus crucial.

Photoelectron spectroscopy (PES) has already played a major role in understanding the behavior of the valence band (VB) electrons of Fe₃O₄. At room temperature Fe₃O₄ is a moderately conducting mixed-valent oxide; it has the cubic inverse spinel structure with Fe³⁺ ions (1/3 of the Fe ions) occupying tetrahedral (A) sites and with Fe³⁺, Fe²⁺ ions randomly distributed in equal amount occupying octahedral (B) sites. This ionic description has been used by Néel⁸ to calculate that the $4 \mu_B$ magnetic moment per Fe₃O₄ formula unit is due to the antiferromagnetic coupling of the magnetic moments on the A and B sites, which was

established later by neutron diffraction.⁹ Most of the early PES investigations of the Fe₃O₄ VB (Ref. 10 and references therein) have been interpreted using this ionic model, which accounts satisfactorily for the presence of O $2p$ -derived states in the 3–8 eV binding energy (BE) range and of Fe $3d$ -derived states extending over 4 eV below the Fermi level (E_F).

Another description of Fe₃O₄ VB states relies on band-structure calculations, which predict band dispersion of Fe(B) t_{2g} states near E_F ^{3,4} and a half-metallic behavior with a semiconducting (1.4 eV band gap) majority-spin channel and a conductive minority-spin channel, resulting in a 100% spin polarization at E_F .⁴ So, clear experimental characterization of the t_{2g} band, populated by the “extra” electron of the B site Fe²⁺ ion, is of major interest for technological application of Fe₃O₄.

In the past, the electronic structure of Fe₃O₄ has mostly been investigated by normal emission PES.^{10,11} Siratori *et al.*¹² performed the first angle-resolved (AR) PES experiment. No clear evidence of band dispersion was observed, but it was concluded that the reasonable agreement between the BE of the Fe $3d$ -O $2p$ states found in the experiment and in the calculation available at this time³ advocates for an itinerant-electron description of the Fe₃O₄ VB. In a later ARPES study on a Fe₃O₄(1 1 1) thin film grown on Pt(1 1 1), a dispersion along the ΓL direction of two faint features in the lowest BE range was observed by Cai *et al.*¹¹ and considered by these authors to be qualitatively compatible with the band-structure calculation of Ref. 4. Off-normal PES data recorded at $\hbar\omega = 58$ eV along the $\bar{\Gamma} M$ direction of

the $\text{Fe}_3\text{O}_4(111)$ surface Brillouin zone (BZ) show a strong dispersion of O $2p$ -derived states in the 2.5–8 eV BE range, only a weak, but periodic, dispersion being observed for the Fe $3d$ -derived states near E_F .¹³ This observation led the authors to infer that two different surface BZs needed to be taken into consideration for a full description of the surface electronic band structure of a $\text{Fe}_3\text{O}_4(111)$ film.¹³ Thus, up to now, any agreement of ARPES experiments with the band dispersions predicted by theory for bulk Fe_3O_4 is far from being convincing, in particular as far as the Fe t_{2g} states are concerned.

The spin polarization (SP) of photoelectrons has been used as early as the late 1970s to investigate the magnetic properties of Fe_3O_4 by Alvarado *et al.*¹⁴ These authors reported a SP of -60% at ~ 2 eV BE in a Fe_3O_4 single crystal held at 10 K. More recently many efforts have been made to test for the half-metallicity of Fe_3O_4 using spin-resolved (SR) PES. A SP polarization at E_F as high as $-(80 \pm 5)\%$ has been measured on the (111) surface at room temperature, which has been considered as evidence of the HM nature of Fe_3O_4 in the (111) direction.¹⁵ But, for the $\text{Fe}_3\text{O}_4(100)$ thin films grown on $\text{MgO}(100)$, the SP measured by SRPES was only $-(40\text{--}55)\%$ near E_F .^{16–18} Surface imperfections and strong electron correlation effects were invoked to explain this low value for the (100) surface. These discrepancies are also due to the fact that truncations of the Fe_3O_4 crystal are polar. Therefore they are very sensitive not only to the experimental preparation conditions but also to the entire thermochemical history and are unstable in an unreconstructed state, leading to the coexistence of different structures on the same surface. Later, Tobin *et al.*¹⁹ have reported SRPES results obtained using photon energies higher than those traditionally used in these kinds of experiments in order to minimize the role of the disrupted surface layer and to be able to measure the bulk SP of “as received” samples. However, despite the higher kinetic energies of the photoelectrons, they do not observe a full SP at E_F which lead them to conclude that Fe_3O_4 is not a HM. This point of view has later been disputed by Fomin *et al.*²⁰ Thus no definite conclusion emerges.

To summarize, the localized versus itinerant picture of Fe_3O_4 VB states as well as the HM character of Fe_3O_4 remain open questions, which appeal for new experimental investigations.

In this paper we report ARPES and SRPES measurements on $\text{Fe}_3\text{O}_4(001)/\text{MgO}(001)$ films. Although the PES intensity at E_F is very low because of the role played by polarons, a dispersion of the Fe t_{2g} states and a Fermi surface (FS) are observed. The states close to E_F show a high SP, which varies with photon energy mainly due to change in the probing depth and to intrinsic processes, such as photohole lifetime contribution. These various experimental data can be reproduced consistently starting from GGA + U band-structure calculations. They demonstrate that Fe_3O_4 can be described by a band model and strongly support its HM nature.

II. METHODS

The ARPES spectra on $\text{Fe}_3\text{O}_4(001)$ thin films (~ 50 nm thick) epitaxially grown *in situ* on $\text{MgO}(100)$ were acquired at the SOLEIL synchrotron radiation facility on the Cassiopée

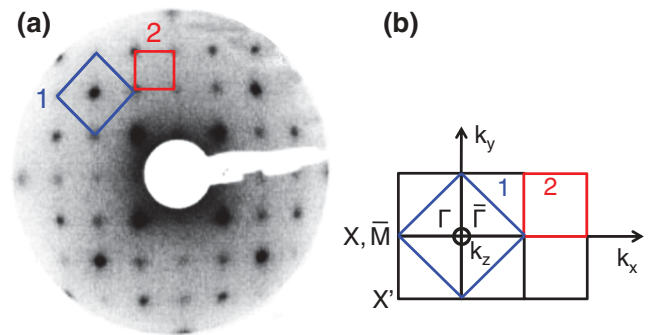


FIG. 1. (Color online) (a) Typical LEED pattern of a $\text{Fe}_3\text{O}_4(001)$ film grown on $\text{MgO}(001)$. (b) Scheme of the reciprocal space. k_z and k_y refer to normal emission and ARPES experiments parallel to the ΓX $[010]$ bulk direction, respectively. The pattern of the bulk primitive lattice is marked by the blue square (1) and the $(\sqrt{2} \times \sqrt{2})R45^\circ$ reconstruction by the red square (2).

beamline; the overall experimental energy resolution is 100 meV as a consequence of the measurements being performed at room temperature and the angular resolution is better than 0.5° . As discussed below, this energy resolution is sufficient because of the presence of intrinsic (electron-lattice) interactions that induce a broadening of ~ 600 meV in the case of Fe_3O_4 .²¹ The Fe_3O_4 lattice constant (8.396 Å) is very closely (0.3%) twice that of MgO (4.211 Å), so there is a small mismatch during epitaxial growth. Both MgO and Fe_3O_4 structures are based on a fcc O^{2-} lattice, allowing a continuation of the oxygen sublattice across their interface. Prior to Fe deposition at a 0.1 nm/min rate under an O_2 pressure of 10^{-6} mbar, the MgO substrate was annealed at 600°C for 2 h to remove surface contamination. During the growth, MgO was held at 300°C , a temperature low enough to prevent Mg interdiffusion.^{22,23} After growth, the films were *in situ* characterized by low energy electron diffraction (LEED) and x-ray ($\text{Al } K\alpha$) photoelectron spectroscopy. LEED spots were observed down to an energy of 17 eV, which is an indication of the high crystalline quality of the films. This is also confirmed by the fact that we have observed by PES the opening of a (100 ± 10) meV gap close to E_F at (125 ± 10) K, characteristic of the apparition of the low temperature semiconducting phase below the Verwey temperature (~ 122 K in Fe_3O_4 single crystals).²⁴

Figure 1(a) shows a LEED pattern (electron energy of 69 eV) of the $\text{Fe}_3\text{O}_4(001)$ surface exhibiting the well known²⁵ and now fully understood²⁶ $(\sqrt{2} \times \sqrt{2})R45^\circ$ reconstruction. Blue and red squares indicate the primitive (1×1) and $(\sqrt{2} \times \sqrt{2})R45^\circ$ lattices, respectively. The reciprocal space is given in Fig. 1(b), where Γ , X , and X' , and $\bar{\Gamma}$ and \bar{M} are high symmetry points of the bulk and the surface BZ, respectively. The k_z axis represents normal emission of electrons, whereas the k_y axis stands for angle-dependent measurements.

The SRPES measurements were done using a time-of-flight electron analyzer collecting the electrons at normal emission, equipped with a Mott polarimeter.²⁷ Barium borate crystals were used for phase-matched harmonic generation of 4.65 and 6.20 eV photons from the 250 kHz Ti:sapphire laser source of the T-ReX laboratory (FERMI@Elettra, Trieste). In this

case, the measurements necessitated sample transfer in air. No cleaning procedure has been used prior to the measurement. After completion of the SRPES measurements, a LEED pattern was still present. This confirms the feasibility of using *ex situ* prepared Fe_3O_4 samples in PES investigations.¹⁹

Fe $2p$ x-ray magnetic circular dichroism (XMCD) spectra were recorded in the analysis chamber of the BACH beamline of the Elettra synchrotron light laboratory. The XMCD spectra were in excellent agreement with those previously considered to be representative of Fe_3O_4 samples.²⁸

All spectra were recorded under a vacuum lower than 5×10^{-10} mbar at room temperature on films in remanent state. The magnetization was performed *ex situ* along the (110) axis with a permanent magnet.

Band calculations²⁹ were performed using the full-potential augmented plane wave + local orbital method with the generalized gradient approximation including an effective Hubbard term (GGA + U)³⁰ to account for the strong localization of the Fe $3d$ states.

III. RESULTS AND DISCUSSION

A. Fe t_{2g} band dispersion

Figure 2(a) shows a set of VB PES spectra recorded in normal emission, i.e., along the ΓX line of the bulk BZ, with photon energies $\hbar\omega$ in the 100–200 eV range. Each spectrum is normalized to its integrated intensity. According to our calculations and also to Refs. 3–5, the features located in the 0–3 eV and in the 3–8 eV BE range are due to Fe $3d$ - and the O $2p$ -derived states, respectively.

The t_{2g} band, due to electrons from B-site Fe^{2+} ions, is expected to lie between E_F and a BE of ~ 0.8 eV as indicated by dotted lines in Fig. 2(a). Figure 2(b) shows an expanded view of this region. Neither a clear Fermi edge nor a dispersion can be observed. This is in contradiction with band calculations that predict a metallic state, but is similar to what has been observed in previous experiments.^{13,17–20,31–36}

The absence of spectral weight at E_F can be explained by strong electron-lattice coupling, along the lines of the interpre-

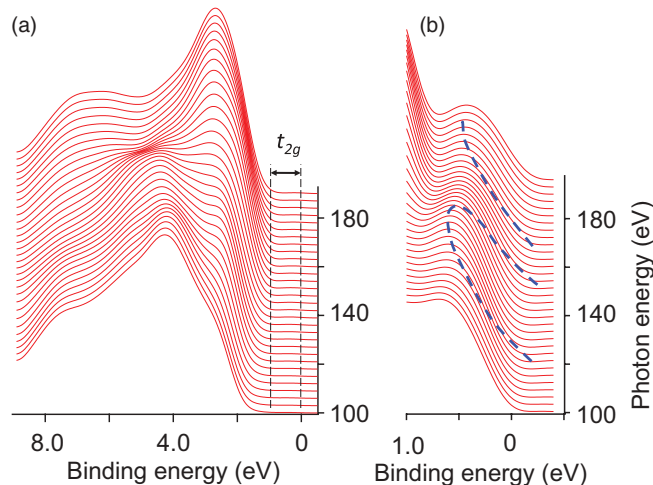


FIG. 2. (Color online) (a) Normal emission valence-band spectra. (b) Detail of the t_{2g} band on expanded intensity and energy scales. The blue dashed line is a guide to the eye indicating the band dispersion expected from our calculations.

tation of VB PES spectra of many transition metal oxides.³⁷ When an electron is removed from such a coupled system, the PES spectrum consists of a coherent quasiparticle peak, whose spectral weight is greatly reduced and renormalized in energy, and of an incoherent background of sidebands shifted away from E_F . The electron-lattice interaction, described in the model of small polarons, is so strong in Fe_3O_4 ³⁸ that the intensity of the quasiparticle peak is completely washed out.³⁷ As Fe_3O_4 is a ferrimagnet, the photohole (a spin-1/2 object) can also be dressed by spin wave excitations and therefore can also decay into a spin polaron.³⁹

An important aspect of the fermion-boson interaction model is that the first moment of the spectral weight remains peaked at the frozen-lattice electronic energy.^{37,40} Thus we attribute the hump at ~ 0.6 eV BE in Fig. 2(b) to sidebands of quasiparticles strongly dressed by polarons.

To reveal any weak features that might be present close to E_F , we display in Fig. 3(a) the second derivative of the raw data. Now a clear dispersion appears as an arc (blue) crossing E_F . Another dispersive arc crossing E_F starts at $\hbar\omega \sim 195$ eV; its evolution is however beyond the $\hbar\omega$ range used. The upper panel of Fig. 3(a) shows photoemission intensity variation at E_F . Referring to our band-structure calculations, the highest BE of the dispersion arc found for $\hbar\omega \sim 133$ eV can be attributed to the Γ point. Using the free-electron approximation for the final state, which is satisfactory for our photoelectron kinetic energy range, we find a value of

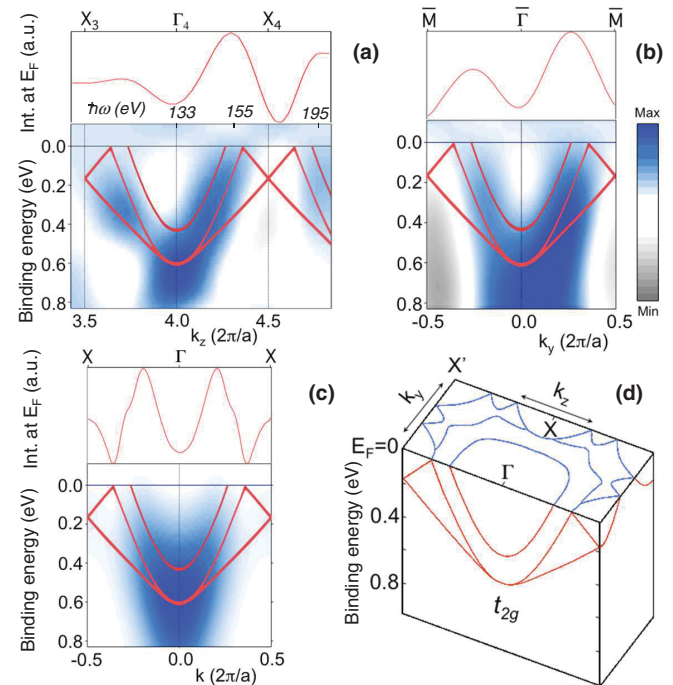


FIG. 3. (Color online) Intensity plots of the second derivative of the PES data showing the Fe t_{2g} band dispersion: (a) along ΓX and (b) along $\bar{\Gamma} \bar{M}$ in the surface BZ [see Fig. 1(b)]. (c) Simulation of the experimental data (see text for details). The upper part of (a)–(c) shows the spectral weight variation at E_F . The GGA + U t_{2g} band is superimposed as red lines. (d) Three-dimensional view of the GGA + U calculation. The ground state Fermi surface is shown in blue.

4 eV for the inner potential V_0 , defined by $k \propto \sqrt{\hbar\omega + V_0}$; consequently the dispersion in the k_z direction is located in the third and fourth BZ. In Fig. 3(a) the t_{2g} band given by our GGA + U calculation is also shown (red lines) and is superimposed on the second derivative plot. We found that $U = 2.7$ eV leads to the best compromise for fitting the band dispersion and, as discussed in the following, the FS and the SP as well. The ~ 0.6 eV amplitude of the dispersion agrees well with theory. The dispersion we observe has a rather broad width; this is due to the extremely low signal close to E_F which makes it difficult to obtain a sharp contrast, even using a second derivative representation. Dispersive arcs were present in all the spectra of the various samples we have studied, which excludes the possibility of a film quality issue.

For the (111) surface, a faint t_{2g} band dispersion was observed in Ref. 11, where it was considered that the humps in the PES spectra correspond to bare electron dispersion; note however that no E_F crossing by a band was observed. The assignment of the hump to the electronic band was rather intuitive because a theoretical support of this fact came much later.^{37,40} It should also be mentioned that the (111) surface is not reconstructed, rendering the comparison of experiment with electronic structure calculation for the bulk material more straightforward.

A contribution from the surface electronic structure is to be expected since PES is a surface sensitive technique. A periodicity of the surface reconstruction can be obtained when measuring electron emission at a fixed photon energy in angular dispersion. The most appropriate is to choose $\hbar\omega = 133$ eV for which we have identified the Γ_4 point of the bulk BZ. Then the Γ_4 and $\bar{\Gamma}$ points as well as the $X_{3,4}$ and \bar{M} points are superimposed and the spectra are measured along the [010] (k_y) direction [Fig. 1(b)]. The results are displayed in Fig. 3(b). We observe the same clear dispersion as in Fig. 3(a), with the same BE amplitude, again in agreement with the theoretical bands. It is remarkable that we observe bulk bands in spite of the $(\sqrt{2} \times \sqrt{2})R45^\circ$ reconstruction. When looking for a signature of surface states one needs to keep in mind that in our experimental geometry, measuring parallel to the Γ -X direction, the (001) surface reconstruction is arranged in such a way that in reciprocal space [Fig. 1(b)] its BZ is half of that corresponding to the bulk crystal. As a matter of fact, we observe both periodicities, i.e., one corresponding to 8.4 Å (conventional fcc lattice) and another to 4.2 Å (primitive lattice), in the intensity profile at E_F [upper panel of Fig. 3(b)]. In addition, this intensity profile shows the same features as the one drawn for the perpendicular emission study [upper panel of Fig. 3(a)]. As a conclusion we note that the t_{2g} band is folded in such a way that it crosses E_F at the edges of the surface BZ. In other words, the presence of surface states with a periodicity of the reconstruction cannot be excluded from our data but it cannot be deduced either.

Thus, as seen, the overall behavior of the energy bands is in very good agreement with our calculations. Because at present the calculation of PES spectra is hardly feasible for complex systems such as Fe_3O_4 ,⁴¹ we did a simulation of the spectra using a simple model. We used the free-electron approximation for the final states, completely ignoring the matrix elements. In the simulation the ground state bands were convoluted

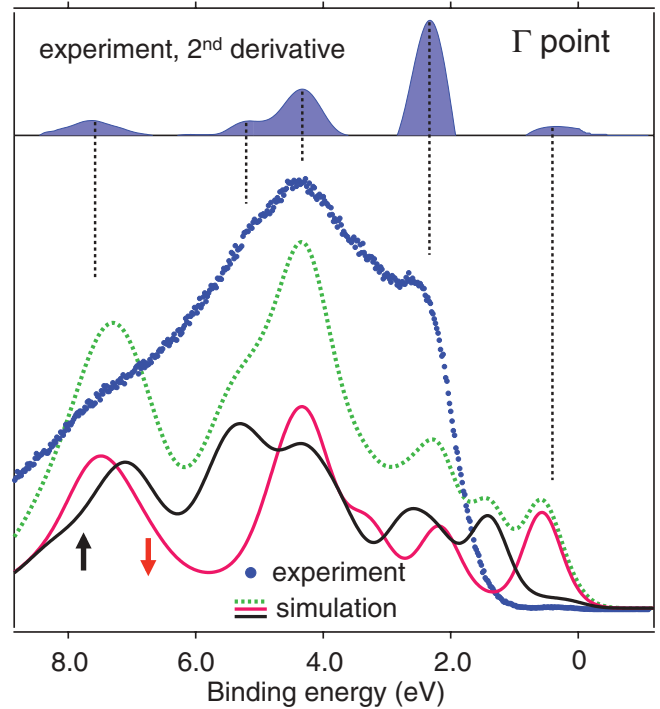


FIG. 4. (Color online) Photoemission spectrum at the Γ point (blue dots) and its second derivative (upper panel). Vertical dotted lines indicated positions of main structures in the spectrum. Simulation of the experimental data is shown as a green dotted line. Red and black full lines represent simulated contribution of spin-down and spin-up electrons, respectively.

by Lorentzian and Gaussian³⁷ functions to account for the initial-state lifetime broadening and electron-lattice coupling effects, respectively. The full width at half maximum of the Lorentzian (FWHM_L) was assumed to vary linearly from 0 at E_F to 1.2 eV at 12 eV BE, which covers the whole VB width, in a similar way as done in Ref. 42; that of the Gaussian was taken²¹ as $\text{FWHM}_G = 600$ meV. In three-dimensional systems, like Fe_3O_4 , in the interpretation of ARPES data one needs to take into account also the intrinsic broadening of the electron momentum component perpendicular to the crystal surface k_\perp .⁴³ However, when introduced in the simulation, this brought only a subtle additional smearing of spectral features as compared to the contribution of polarons. So, in the following, it will not be taken into account. The result of the simulation is shown in Fig. 3(c) and for illustration, a three-dimensional view of the GGA + U-calculated bands is plotted in Fig. 3(d).

The adequacy of the proposed model can be better tested on a single photoemission spectrum as demonstrated in Fig. 4 where we show a spectrum (blue dots) and its second derivative (upper panel) measured at the Γ point. As we have neglected matrix elements, only a comparison of the BE of the main structures in the spectrum between theory and experiment is relevant. These are well reproduced in the simulation (green dotted line). Moreover, partial contribution of spin-up (black full line) and spin-down (red full line) electrons allow us to anticipate the expectation value of the SP, as it will be discussed in Sec. III C.

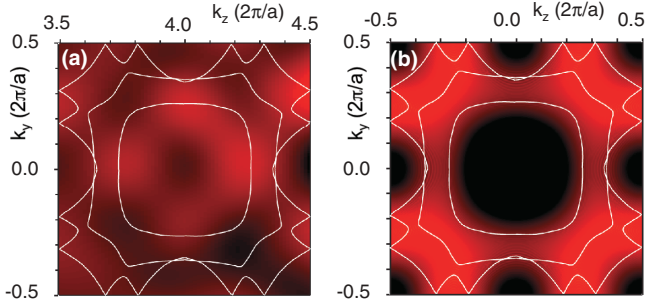


FIG. 5. (Color online) Intensity plots of the FS. The white lines show the contours predicted by our GGA + U calculation. (a) Second derivative of the PES intensity over a 100 meV interval at E_F . (b) Simulation using the same parameters as in Fig. 3(c).

B. Fermi surface

By integrating the spectral intensity over an energy interval of 100 meV at E_F , a FS plot is obtained and in Fig. 5(a) we show the two-dimensional second derivative of it. Although its presence has been predicted by theory, we report here experimental evidence of this FS. This FS is simply a replica of that of the bare electrons (in a rigid lattice) but with a strongly reduced intensity at E_F . It is to be noted that the measured FS plot is presented here in an unconventional way, as k_z represents bulk electronic properties and k_y the surface properties. This gives us the possibility to unravel differences between surface and bulk electronic structure. Surprisingly, both contributions give the same symmetries and periodicities indicating again the fact that the influence of the surface states is negligible. The symmetry of the experimental FS is in quite good agreement with that obtained from the calculated band structure (superimposed white lines). We also performed a simulation of the FS using the procedure and the parameters mentioned previously [Fig. 5(b)]. A qualitative agreement with the experiment is achieved especially in the corners of the BZ. In the central part of the BZ there is an apparent discrepancy between experiment and simulation. Clearly, in this case, our simple model is unable to describe the spectral intensity distribution through the whole BZ. This might be due to a strong anisotropy of the polaron interaction^{37,44} giving rise to intensity enhancement approximately in the middle of the ΓX high symmetry axis, i.e., where the bands cross E_F at almost the same k points.

C. Spin polarization

Determination of the SP is an ultimate test of both the band calculations and our method of simulating Fe₃O₄ PES spectra. Here it is worth noting that the same sample was used as for spin-integrated ARPES, requesting its transfer through air to another chamber. The sample was not subject to any cleaning procedure prior to the SRPES measurements, which logically leads to a reduction of the SP as a consequence of the presence of a dead layer (contamination, nonstoichiometric composition) on the surface. In spite of this fact, the SP close to E_F reaches -50% and -72% for 6.20 and 4.65 eV photons, respectively, as shown in the upper panel of Fig. 6(a).

Our results can be compared to those for an *in situ* prepared (001) surface for which a SP of -55% was reported,²⁰ the

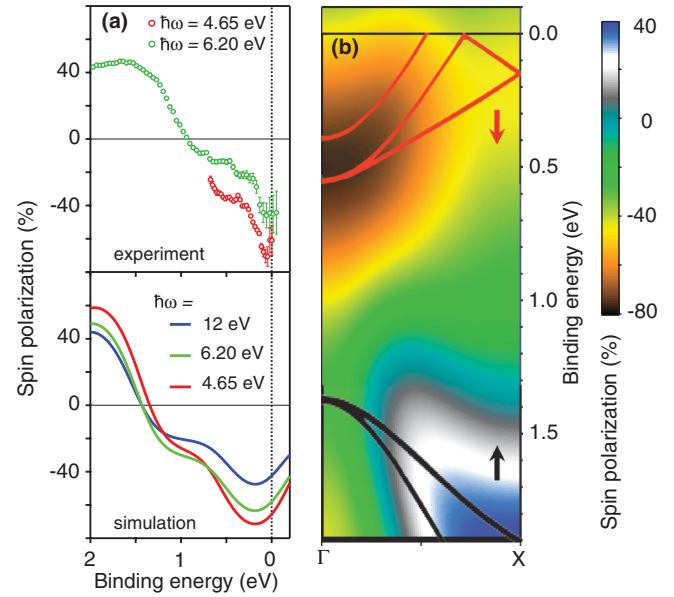


FIG. 6. (Color online) (a) SP deduced from SR- and AR-PES at normal emission using $\hbar\omega = 4.65$ and 6.20 eV (upper panel); the spin-polarized spectrum (blue line) at the X point (lower panel) extracted from (b). Simulations (see text for details) for $\hbar\omega = 6.20$ (green line) and 4.65 eV (red line) are shown for comparison. (b) Simulation of the SP in the ΓX plane for $\hbar\omega = 12$ eV. Red and black lines are, respectively, spin-down and spin-up bands.

maximum value ever reported for this surface before the present study. The reduction of the SP as compared to a HM is explained by the surface reconstruction leading to lattice distortions⁴⁵ and consequently to changes in the electronic properties. To our knowledge, the only calculation of the electronic structure of the reconstructed surface³¹ is unable to give a clear description of it.

In a first approach, the high value of SP we observe can be explained by an increase in the inelastic mean-free path when lowering $\hbar\omega$, which probes bulk properties more efficiently. The simulation of the SP in the ΓX plane, using the same parameters as before, is shown in Fig. 6(b). Namely, the convolution by the Lorentzian spreads out up to 12 eV BE, i.e., through the whole VB. Spin-down and spin-up bands are superimposed on the SP intensity plot as red and black lines, respectively. Clearly our SP measurements are consistent with the bandlike description as seen from the comparison between the simulated spin-polarized spectrum at the X point [blue line in the lower panel of Fig. 6(a)], extracted from the ΓX plot, and the measurement. Both the maximum negative SP value and the point of SP reversal are well reproduced.

Interestingly, the measured SP marks a considerable increase at $\hbar\omega = 4.65$ eV, not accounted for in our simple model. At first sight, only the argument of electron mean-free path can be put forward to justify this increase because, as seen in Fig. 6(b), the simulated SP dispersion is rather flat and changing $\hbar\omega$ from 6.20 to 4.65 eV corresponds to the k -vector variation of only $\sim 15\%$ of the Brillouin zone in the ΓX direction. This cannot justify the increase from $\sim -50\%$ to $\sim -70\%$. However, it should be borne in mind that our simulation takes into account the energy dependence of the

initial-state lifetime broadening across the whole VB width, i.e., as if performed using “standard” PES photon energies ($\hbar\omega > 12$ eV). In such a situation, as the width of the photohole is large at high BE, it brings a contribution at E_F from deeper lying spin-up bands. This results in an important mixing of states at E_F and consequently in a washing out of the spin contrast (see also Fig. 4). This is a crucial point for the interpretation of spin-polarized data as measured by PES. It indicates that due to intrinsic phenomena, such as the initial lifetime, it is impossible to measure 100% polarized electrons in a half-metal.

In order to take into account that $\hbar\omega$ is smaller than 12 eV, and therefore only holes up to a BE given by $(E_F - \hbar\omega)$ contribute to the initial state broadening, we did the convolution with the Lorentzian up to the same value of the BE as the energy of the impinging laser light. Now, the simulations fit better the experimental SP [see Fig. 6(a), lower panel: green and red lines].

Pushing these considerations further on allows us to assert that in electronic devices using electric current, i.e., where only electrons in the vicinity of E_F are excited, a SP close to -100% is to be expected. The polaron contribution will be of a limited amount because its energy width (~ 0.6 eV) is much

smaller than the majority spin gap in Fe_3O_4 (~ 1.4 eV) and because the bosonic degrees of freedom do not affect the spin.

IV. SUMMARY

In conclusion, we have determined, by photoemission measurements, three main characteristics of the electronic structure of Fe_3O_4 : Fe t_{2g} band dispersion in the vicinity of E_F , Fermi surface, and spin polarization. These three sets of photoemission data can be simulated starting from GGA + U bulk band-structure calculations and taking into account the polaron and initial-state lifetime broadening involved in the photoemission process. Our results conciliate the electronic structure of Fe_3O_4 with a band model and, more specifically, confirm that magnetite is a half-metal.

ACKNOWLEDGMENTS

The research leading to these results has received funding from the European Community’s Seventh Framework Program (FP7/2007-2013) under Grant Agreement No. 226716. P.B. was supported by the Austrian Science Foundation FWF (SFB-F41).

-
- ¹J. P. Velev, S. S. Jaswal, and E. Y. Tsymbal, *Philos. Trans. R. Soc. London Sect. A* **369**, 3069 (2011).
- ²H. Y. Hwang, Y. Iwasa, M. Kawasaki, B. Keimer, N. Nagaosa, and Y. Tokura, *Nat. Mater.* **11**, 103 (2012).
- ³A. Yanase and K. Siratori, *J. Phys. Soc. Jpn.* **53**, 312 (1984).
- ⁴Z. Zhang and S. Satpathy, *Phys. Rev. B* **44**, 13319 (1991).
- ⁵A. Yanase and N. Hamada, *J. Phys. Soc. Jpn.* **68**, 1607 (1999).
- ⁶C. Felser, G. H. Fecher, and B. Balke, *Angew. Chem. Int. Ed.* **46**, 668 (2007).
- ⁷R. Ramesh and S. A. Spaldin, *Nat. Mater.* **6**, 21 (2007).
- ⁸L. Néel, *Ann. Phys. (Paris)* **3**, 137 (1948).
- ⁹C. G. Shull, E. O. Wollan, and W. A. Strauser, *Phys. Rev.* **81**, 483 (1951).
- ¹⁰R. J. Lad and V. E. Henrich, *Phys. Rev. B* **39**, 13478 (1989).
- ¹¹Y. Q. Cai, M. Ritter, W. Weiss, and A. M. Bradshaw, *Phys. Rev. B* **58**, 5043 (1998). In this reference the ARPES data are compared to the calculation of Ref. 3.
- ¹²K. Siratori, S. Suga, M. Taniguchi, K. Soda, S. Kimura, and A. Yanase, *J. Phys. Soc. Jpn.* **55**, 690 (1986).
- ¹³Yu. S. Dedkov, M. Fonin, D. V. Vyalikh, J. O. Hauch, S. L. Molodtsov, U. Rüdiger, and G. Güntherodt, *Phys. Rev. B* **70**, 073405 (2004).
- ¹⁴F. Alvarado, W. Eib, F. Meier, D. T. Pierce, K. Sattler, H. C. Siegmann, and J. P. Remeika, *Phys. Rev. Lett.* **34**, 319 (1975).
- ¹⁵Yu. S. Dedkov, U. Rüdiger, and G. Güntherodt, *Phys. Rev. B* **65**, 064417 (2002).
- ¹⁶D. J. Huang, C. F. Chang, J. Chen, L. H. Tjeng, A. D. Rata, W. P. Wu, S. C. Chung, H. J. Lin, T. Hibma, and C. T. Chen, *J. Magn. Magn. Mater.* **239**, 261 (2002).
- ¹⁷S. A. Morton, G. D. Waddill, S. Kim, I. K. Schuller, S. A. Chambers, and J. G. Tobin, *Surf. Sci.* **513**, L451 (2002).
- ¹⁸E. Vescovo, H.-J. Kim, J. M. Ablett, and S. A. Chambers, *J. Appl. Phys.* **98**, 084507 (2005).
- ¹⁹J. G. Tobin, S. A. Morton, S. W. Yu, G. D. Waddill, I. K. Schuller, and S. A. Chambers, *J. Phys.: Condens. Matter* **19**, 315218 (2007).
- ²⁰M. Fonin, Yu. S. Dedkov, R. Pentcheva, U. Rüdiger, and G. Güntherodt, *J. Phys.: Condens. Matter* **20**, 142201 (2008).
- ²¹S. K. Park, T. Ishikawa, and Y. Tokura, *Phys. Rev. B* **58**, 3717 (1998).
- ²²J. F. Anderson, M. Kuhn, U. Diebold, K. Shaw, P. Stoyanov, and D. Lind, *Phys. Rev. B* **56**, 9902 (1997).
- ²³N. Spiridis, B. Handke, T. Slezak, J. Barbasz, M. Zajac, J. Haber, and J. Korecki, *J. Phys. Chem. B* **108**, 14356 (2004).
- ²⁴A. Chainani, T. Yokoya, T. Morimoto, T. Takahashi, and S. Todo, *Phys. Rev. B* **51**, 17976 (1995).
- ²⁵S. A. Chambers and S. A. Joyce, *Surf. Sci.* **420**, 111 (1999).
- ²⁶R. Pentcheva, W. Moritz, J. Rundgren, S. Frank, D. Schrupp, and M. Scheffler, *Surf. Sci.* **602**, 1299 (2008).
- ²⁷C. M. Cacho, S. Vlais, M. Malvestuto, B. Ressel, E. A. Seddon, and F. Parmigiani, *Rev. Sci. Instrum.* **80**, 043904 (2009).
- ²⁸D. J. Huang, C. F. Chang, H.-T. Jeng, G. Y. Guo, H.-J. Lin, W. B. Wu, H. C. Ku, A. Fujimori, Y. Takahashi, and C. T. Chen, *Phys. Rev. Lett.* **93**, 077204 (2004).
- ²⁹P. Blaha, K. Schwarz, G. K. H. Madsen, D. Kvasnicka, and J. Luitz, *WIEN2k, An Augmented Plane Wave + Local Orbitals Program for Calculating Crystal Properties* (K. Schwarz, Technische Universität, Wien, 2008).
- ³⁰V. I. Anisimov, I. S. Elfimov, N. Hamada, and K. Terakura, *Phys. Rev. B* **54**, 4387 (1996).
- ³¹M. Fonin, R. Pentcheva, Yu. S. Dedkov, M. Sperlich, D. V. Vyalikh, M. Scheffler, U. Rüdiger, and G. Güntherodt, *Phys. Rev. B* **72**, 104436 (2005).
- ³²M. Fonin, Yu. S. Dedkov, J. Mayer, U. Rüdiger, and G. Güntherodt, *Phys. Rev. B* **68**, 045414 (2003).
- ³³Yu. S. Dedkov, M. Fonin, U. Rüdiger, and G. Güntherodt, *Appl. Phys. A* **82**, 489 (2006).

- ³⁴M. Fonin, Yu. S. Dedkov, R. Pentcheva, U. Rüdiger, and G. Güntherodt, *J. Phys.: Condens. Matter* **19**, 315217 (2007).
- ³⁵D. Schrupp, M. Sing, M. Tsunekawa, H. Fujiwara, S. Kasai, A. Sekiyama, S. Suga, T. Muro, V. A. M. Brabers, and R. Claessen, *Europhys. Lett.* **75**, 075115 (2007).
- ³⁶M. Kimura, H. Fujiwara, A. Sekiyama, J. Yamaguchi, K. Kishimoto, H. Sugiyama, G. Funabashi, S. Imada, S. Iguchi, Y. Tokura, A. Higashiya, M. Yabashi, K. Tamasaku, T. Ishikawa, T. Ito, S. Kimura, and S. Suga, *J. Phys. Soc. Jpn.* **79**, 064710 (2010).
- ³⁷K. M. Shen, F. Ronning, W. Meevasana, D. H. Lu, N. J. C. Ingle, F. Baumberger, W. S. Lee, L. L. Miller, Y. Kohsaka, M. Azuma, M. Takano, H. Takagi, and Z.-X. Shen, *Phys. Rev. B* **75**, 075115 (2007).
- ³⁸D. Ihle and B. Lorenz, *J. Phys. C* **18**, L647 (1985).
- ³⁹J. Chaloupka and G. Khaliullin, *Phys. Rev. Lett.* **99**, 256406 (2007).
- ⁴⁰A. S. Mishchenko, *Adv. Condens. Matter Phys.* **2010**, 306106 (2010).
- ⁴¹J. Minár, J. Braun, S. Mankovsky, and H. Ebert, *J. Electron Spectrosc. Relat. Phenom.* **184**, 91 (2011).
- ⁴²J. Krempaský, V. N. Strocov, L. Patthey, P. R. Willmott, R. Herger, M. Falub, P. Blaha, M. Hoesch, V. Petrov, M. C. Richter, O. Heckmann, and K. Hricovini, *Phys. Rev. B* **77**, 165120 (2008).
- ⁴³V. N. Strocov, *J. Electron Spectrosc. Relat. Phenom.* **130**, 65 (2003).
- ⁴⁴V. Perebeinos and P. B. Allen, *Phys. Rev. Lett.* **85**, 5178 (2000).
- ⁴⁵R. Pentcheva, F. Wendler, H. L. Meyerheim, W. Moritz, N. Jedrecy, and M. Scheffler, *Phys. Rev. Lett.* **94**, 126101 (2005).